Manuscript Details

Manuscript number	MARGO_2019_360
Title	Origin of manganese in coccolith calcite based on synchrotron nanoXRF and XANES
Article type	Research Paper

Abstract

Calcareous nannofossils are small (~1-15 µm) calcite platelets produced by coccolithophores (i.e., coccoliths), photosynthetic algae, and some incertae sedis also called calcareous nannoplankton. Coccolithophores inhabit the photic zone from coast to open-oceanic realms and, associated with the calcareous nannofossils, have an abundant fossil record down to the Late Triassic. Hence it may be an interesting material for geochemically-based paleoenvironmental reconstructions that has clearly been overlooked to the exception of the Sr/Ca as a proxy for productivity. In this study, we have analyzed manganese (Mn) distribution and valence in several species of calcareous nannofossils from different ages (i.e., recent to Jurassic) and localities (i.e., sections in Portugal and USA, core-tops from Atlantic and Pacific) and with different ultrastructures in order to test the potential of Mn as a paleobiological or paleoenvironmental proxy. NanoXRF maps were collected at the ESRF IB ID22 and ID21 beamlines as well as Mn K-edge XANES at ID21. Mn is more abundant in coccoliths from section samples (i.e., Jurassic and Paleogene) than in core-tops samples (i.e., recent). In fossil samples, Mn nanoXRF maps show distributions related to primary crystalline organization whereas in core-tops samples Mn distributions are, when present, not constrained by the coccolith crystal lattice. XANES analyses show that Mn is likely in the form of $MnCO_3$. All these observations argue for Mn incorporation within calcareous nannofossils controlled by diagenesis. Advanced diagenesis and calcite encrusting result in secondary Mn-enriched calcite following the original crystals growth directions. Still, the incorporation of Mn in some core-tops samples highlights potential early diagenesis input when the nannofossil is on the seafloor or even possibly in the water column. Hence, like for foraminifera, Mn should be considered as a critical tool to identify diagenetic overgrowth rather than primary environmental conditions.

Keywords	pelagic sediments; micropaleontology (nannos); diagenesis (sea floor); nanoX-ray fluorescence; XANES; microfossil geochemistry
Taxonomy	Diagenesis, Microfossil, Microfossil Geochemistry, X-Ray Fluorescence
Corresponding Author	Baptiste Suchéras-Marx
Corresponding Author's Institution	Aix–Marseille University, CNRS, IRD, CEREGE UM34
Order of Authors	Baptiste Suchéras-Marx, Fabienne Giraud, Isabelle Daniel, Camille RIVARD, Marie Aubry, Karl-Heinz Baumann, Luc Beaufort, Rémi Tucoulou, Alexandre Simionovici
Suggested reviewers	Tom Dunkley Jones, Heather Stoll, Rosalind Rickaby, Silvia Gardin, Michael Hermoso, Susan Louise Svane Stipp

Submission Files Included in this PDF

File Name [File Type]

Cover_letter_Mn_coccolith.docx [Cover Letter]

Highlights.docx [Highlights]

manuscript_submitted.docx [Manuscript File]

Fig1.tif [Figure]

Fig2.tif [Figure]

Fig3.tif [Figure]

Fig4.tif [Figure]

Fig5.tif [Figure]

SupplFig.tif [Figure]

Table1.pdf [Table]

Table2.pdf [Table]

To view all the submission files, including those not included in the PDF, click on the manuscript title on your EVISE Homepage, then click 'Download zip file'.

Research Data Related to this Submission

There are no linked research data sets for this submission. The following reason is given:
I will submit the data in an open repository but, because it is synchrotron data, I need time to discuss with the repository about what they wish.

Dr. Baptiste Suchéras-Marx
Associate lecturer
Aix*Marseille université
CEREGE UM34
Avenue Louis Philibert – Europôle de l'Arbois
13545 Aix-en-Provence
France
sucheras-marx@cerege.fr

Dear *Marine Geology* editor,

On the behalf of my colleagues, I am honored to submit for publication in your journal the present study entitled "*Origin of manganese in coccolith calcite based on synchrotron nanoXRF and XANES*".

The present manuscript focuses on **coccolith and nannofossil chemical composition** and more precisely on **manganese**. Coccoliths – micrometric $CaCO_3$ platelets produced by coccolithophore algae – and more generally calcareous nannofossils are the most important pelagic carbonate producers for the past 200 Ma. Found from coastal to open ocean realms and from equatorial to polar seas, calcareous nannoplankton offers the potential to **record past oceanographic conditions** in their tests over the past 200 Ma. However, due to the very small size (~1-15 µm) of calcareous nannofossils, there are still overlooked in geochemically-based paleoenvironmental reconstructions.

In this study, we present for the first time a discussion on the presence of manganese in calcareous nannofossils comparing Middle Jurassic and core-tops samples from various oceanic regions. The association of various time intervals, calcareous nannofossils crystalline organization and samples geographic origins allows us to precisely explore the mechanisms at **the origin of manganese incorporation in calcareous nannofossils**. We used state-of-the-art X-ray methodologies at ESRF namely nanoXRF mapping and high resolution Xanes. We observe that Jurassic fossils are enriched in many elements in comparison to core-tops. Manganese repartition in calcareous nannofossils follows $CaCO_3$ crystals orientations in fossils but is almost absent in core-tops coccoliths. The Xanes suggests clearly that Mn is in the form of $MnCO_3$ in calcareous nannofossils. Overall, we consider that Mn in coccoliths is not incorporated in the calcite lattice during coccolithogenesis but is encrusted on the test during early seafloor diagenesis and burial diagenesis. Hence, Mn in coccoliths should not be used for paleoenvironmental reconstructions.

Our study is one of the rare studies on calcareous nannofossils chemical composition and goes deeper on the manganese topic than one of the unique publication on the topic (Suchéras-Marx et al., 2016). We hope therefore that our study will be consider for publication to *Marine Geology*.

Sincerely yours,
Baptiste Suchéras-Marx on the behalf of co-authors

Authors' contributions
BSM and FG designed the study with the contribution of ID and AS. BSM, FG, ID, AS, CR and RT conducted the analyses on both beamlines at ESRF whereas MPA, KHB and LB provided samples. BSM and AS performed the data treatment. BSM wrote the manuscript with comments from all contributors.

Proposed reviewers

Tom Dunkley Jones
t.dunkleyjones@bham.ac.uk

Silvia Gardin
Silvia.gardin@upmc.fr

Heather Stoll
heather.stoll@erdw.ethz.ch

Michael Hermoso
Michael.hermoso@sorbonne-universite.fr

Rosalind Rickaby
rosalind.rickaby@earth.ox.ac.uk

Susan L.S. Stipp
stipp@geol.ku.dk

Highlights

- Synchrotron-based nanoXRF and Xanes analyses on Middle Jurassic and core-tops coccoliths in order to explore the potential of elemental geochemistry in coccoliths for paleoceanographic reconstructions.
- Middle Jurassic coccoliths are enriched in many elements in comparison to core-tops coccoliths and particularly in Mn.
- Mn in coccoliths is in the form of Mn carbonate and follows coccoliths crystals directions.
- Mn in coccoliths is not an original component by rather incorporated during seafloor and burial diageneses.

Title: Origin of manganese in coccolith calcite based on synchrotron nanoXRF and XANES

Baptiste Suchéras-Marx[1, *], Fabienne Giraud[2, 3], Isabelle Daniel[4], Camille Rivard[5], Marie-Pierre Aubry[6], Karl-Heinz Baumann[7], Luc Beaufort[1], Rémi Tucoulou[5], Alexandre Simionovici[2, 3]

1 Aix Marseille Univ, CNRS, IRD, Coll France, CEREGE UM34, Aix-en-Provence, France

2 Université Grenoble Alpes, ISTerre, Grenoble, France

3 CNRS, ISTerre, Grenoble, France

4 Université de Lyon, Université Lyon 1, Ens de Lyon, CNRS, UMR 5276 Lab. de Géologie de Lyon, Villeurbanne F-69622, France

5 ESRF – The European Synchrotron Radiation Facility, Grenoble Cedex 9, France

6 Department of Earth and Planetary Sciences, Rutgers University, Piscataway NJ 08854, USA

7 Department of Geosciences, University of Bremen, PO Box 330440, 28334 Bremen, Germany

* Corresponding author: sucheras-marx@cerege.fr

Abstract

Calcareous nannofossils are small (~1-15 µm) calcite platelets produced by coccolithophores (i.e., coccoliths), photosynthetic algae, and some *incertae sedis* also called calcareous nannoplankton. Coccolithophores inhabit the photic zone from coast to open-oceanic realms and, associated with the calcareous nannofossils, have an abundant fossil record down to the Late Triassic. Hence it may be an interesting material for geochemically-based paleoenvironmental reconstructions that has clearly been overlooked to the exception of the Sr/Ca as a proxy for productivity. In this study, we have analyzed manganese (Mn) distribution and valence in several species of calcareous nannofossils from different ages (i.e., recent to Jurassic) and localities (i.e., sections in Portugal and USA, core-tops from Atlantic and Pacific) and with different ultrastructures in order to test the potential of Mn as a paleobiological or paleoenvironmental proxy. NanoXRF maps were collected at the ESRF IB ID22 and ID21 beamlines as well as Mn K-edge XANES at ID21. Mn is more abundant in coccoliths from section samples (i.e., Jurassic and Paleogene) than in core-tops samples (i.e., recent). In fossil samples, Mn nanoXRF maps show distributions related to primary crystalline organization whereas in core-tops samples Mn distributions are, when present, not constrained

by the coccolith crystal lattice. XANES analyses show that Mn is likely in the form of $MnCO_3$. All these observations argue for Mn incorporation within calcareous nannofossils controlled by diagenesis. Advanced diagenesis and calcite encrusting result in secondary Mn-enriched calcite following the original crystals growth directions. Still, the incorporation of Mn in some core-tops samples highlights potential early diagenesis input when the nannofossil is on the seafloor or even possibly in the water column. Hence, like for foraminifera, Mn should be considered as a critical tool to identify diagenetic overgrowth rather than primary environmental conditions.

1. Introduction

Calcareous nannofossils are small calcite platelets (1-15 µm) secreted by the calcareous nannoplankton – coccolithophores and other *incertae sedis*. Coccolithophores – and possibly most extinct calcareous nannoplankton – are photosynthetic, living in the photic zone (Winter et al., 1994). The coccolithophores are the most abundant test-producing algae in the open ocean environment. There are also very abundant in more proximal or upwelling environments although they are less abundant than diatoms (Margalef, 1978; Ziveri et al., 1995). Hence, coccolithophores and by analogy extinct calcareous nannoplankton, is a group covering most oceans and seas and living in the sea surface to the photic zone from coastal to oceanic gyres realms (Winter et al., 1994).

The coccolithophores calcite platelets are called coccoliths and are recorded in marine sediments since 220 Ma (Gardin et al., 2012). Although they are rare in the Late Triassic, calcareous nannofossils became more and more abundant through the Jurassic reaching an optimum in the Early Cretaceous (Suchéras-Marx et al., 2019). Coccoliths and calcareous nannofossils are made of low Mg calcite (~0.005 wt %) also depleted in most other elements (Siesser, 1977; Stoll et al., 2001). It is considered that the most concentrated element in coccolith calcite – other than Ca, C and O – is Sr which represents in *Gephyrocapsa huxleyi* (*sensu* Reinhard, 1972; Bendif et al., 2014) around 0.6 wt % of the coccolith (Stoll et al., 2002). The coccolith's Sr/Ca ratio depends on temperature and coccolith growth rate which is function of coccolithophores growth rate; Sr/Ca has been then proposed as a productivity proxy (Stoll et al., 2000; Stoll et al., 2002a; Stoll et al., 2002b).

Coccolith-based geochemical proxies are very poorly developed in comparison to planktic foraminifera even if calcareous nannofossil geological record is longer and cover almost all photic zone conditions from coast to open-ocean environments. This limitation is firstly due to the micrometric size of calcareous nannofossils, limiting monospecific analyses.

Nevertheless, in the past decades, new methodologies have been developed to isolate calcareous nannofossils from bulk sediments (Stoll et al., 2009; Minoletti et al., 2009; Suchéras-Marx et al., 2016a) and to perform elemental geochemical analyses (Stoll et al., 2007; Suchéras-Marx et al., 2016b; Hermoso et al., 2017). In the aim of developing coccolith-based geochemical environmental proxies, we present hereafter a study on manganese (Mn) in coccoliths.

In the oceans, manganese is a fundamental element, which is biologically limiting but always in excess (Bruland and Lohan, 2003). On one hand, Mn is fundamental for photosynthesis, being the key acting element in the oxygen-evolving complex in the photosystem II which photo-oxidizes water leading to the production of protons and electrons for photosynthesis (Dismukes and van Willigen, 2006). This element is more concentrated in coccolithophore organic matter than in green algae (Ho et al., 2003). On the other hand, Mn is known to form MnO complex in calcite tests of foraminifera and has strong affinity with carbonate (Paquette and Reeder, 1995; Pena et al., 2008). We present here a study based on synchrotron nanoXRF mapping and XANES providing Mn distribution maps and valence in several calcareous nannofossil in order to discuss the potential of this element as paleobiological or paleoenvironmental proxy. The samples and species were selected in order to i) compare several ages (i.e., Middle Jurassic, Paleocene, and Holocene), ii) compare several localities (i.e., Portugal, US, South Atlantic, Western Pacific and Norwegian sea), iii) compare several species with different ultrastructure (i.e., different type of placoliths and a multiradiate nannolith) and iv) overcome the limited spot size at ID21 (see section 2.2.2.) by analyzing rather large calcareous nannofossils (i.e., more than 4 μm). Such a large panel should allow identifying the influence of crystalline organization, the geological time interval and possible diagenesis on Mn incorporation in calcareous nannofossils.

2. Materiel and methods

2.1. Sample preparation

The calcareous nannofossils analyzed in this study come from various ages and places and were all picked following Suchéras-Marx et al. (2016a). The nannofossils were selected based on optical criteria using a x400 magnification light microscope. Those from Jurassic and Paleogene sediments (i.e., fossil) having lower preservation than the core-tops (i.e., recent) coccoliths were more challenging. *Watznaueria britannica* and *Discorhabdus striatus* come from the Lower Bajocian (Middle Jurassic) of Cabo Mondego in Portugal. This section which is the reference one for the Aalenian/Bajocian boundary (Pavia and Enay, 1997) corresponds

to limestone/marlstone alternations. Both nannofossils came from marlstone samples, *W. britannica* from the sample CM60 and *D. striatus* from the sample CM9 (see section in Suchéras-Marx et al., 2012) and were mounted on 500 nm-thick silicon nitride (Si_3N_4) windows (Silson Ltd. Southam, UK).

Discoaster araneus comes from a Paleocene section of Wilson Lake (USA), *Helicosphaera carteri* from South Atlantic (GeoB3721-4) and the warm pool in the western Pacific (MD052920) core-tops, *Calcidiscus leptoporus* from a South Atlantic core-top (GeoB3721-4) and *Coccolithus pelagicus* from a Norwegian sea core-top (GIK23066). All these nannofossils were deposited between two 4 µm-thick sheets of Ultralene (SPEX®), a clean and pure polymer. All these information are summarized in Table 1.

2.2. XRF mapping

2.2.1. 17 keV mapping at ID22NI

Both *W. britannica* and *D. striatus* were analyzed using an incident X-ray beam energy of 17 keV at ID22NI beamline (currently replaced by ID16b) at the European Synchrotron Radiation Facility (ESRF, Grenoble, France), with a 100 nm x 100 nm beam spot size focused by an ESRF custom-made Kirkpatrick-Baez double multilayer mirror device and 2 s dwell time per pixel. The detectors were high-count rate twin SII™ Vortex SDD (silicon drift diodes) detectors, capable of counting up to 200 kcps with no saturation and no peak shift or FWHM broadening, when operated below 10% dead time. The maps were made by adjacent pixels of analysis. The beam line set-up and analysis procedure are similar to those used by Suchéras-Marx et al. (2016b).

2.2.2. 7.5 keV mapping at ID21

X-ray fluorescence maps (XRF) and X-ray absorption near edge structure (XANES) spectra were collected on the ID21 X-ray microscopy beamline at the ESRF (Cotte et al. 2017). The beam was monochromatized by a fixed-exit, double crystal Si(111) monochromator. The incident beam was focused to a 230 x 750 nm² using mirrors with Kirkpatrick-Baez geometry. The fluorescence signal was collected using a 10 mm^2 Rontec silicon drift diode detector, located at 69° with respect to the incident beam and at 49° with respect to the surface of the sample. The dead time was between 9% and 15% during analysis and corrected for in ratios calculations. The microscope was operated under vacuum to avoid absorption and scattering from air. *W. britannica*, *D. striatus*, *H. carteri* and *C. pelagicus* were mapped with 400 nm horizontal and vertical steps and 3 s dwell time per pixel, *D. araneus* was mapped with

500 nm horizontal and vertical steps and 3 s dwell time per pixel whereas *C. leptoporus* was mapped with 200 nm horizontal and vertical steps and 1.5 s dwell time per pixel.

2.3. XANES analysis

For Mn K-edge XANES analyses, the monochromator energy was calibrated using the position of the first inflexion of a Mn metallic foil spectrum at 6.5495 keV. The incident beam was focused to a 250 x 820 nm². Three standards were analyzed namely $KMnO_4$, MnO_2 and $MnCO_3$ and four coccoliths were analyzed namely *D. striatus*, *W. britannica*, *D. araneus* and *H. carteri*. For both standards and coccoliths, Mn K-edge XANES were collected on the 6.52-6.60 keV energy range with 0.5 eV step and 50 ms. For standards, this procedure was repeated 10 times whereas for coccoliths it was repeated 50 times. This was a compromise of better statistics while avoiding radiation damage to the samples. The spectra hereafter correspond to the average of all XANES spectra per sample, normalized to the incident flux.

3. Results

3.1. XRF spectra

At 17 keV in *D. striatus* and *W. britannica*, 17 elements were recorded, namely S, Cl, Ar, K, Ca, Ti, V, Cr, Mn, Fe, Cu, Zn, Br, Kr, Rb, Sr and Pb (Fig. 1). Among them, Ar and Kr come from the air of the experimental hutch and Pb is a likely contaminant from experimental hutch shielding. Results are in good agreement with those obtained earlier for *W. britannica* (Suchéras-Marx et al., 2016b). The spectra collected at 7.5 keV provide the distribution of Mg, Na and in *D. striatus* and *W. britannica*; the Si signal mainly comes from the Si_3N_4 membrane (Fig. 2). At 7.5 keV, the XRF spectra of *D. araneus*, *C. leptoporus*, *H. carteri* and *C. pelagicus* differ from those of *D. striatus* and *W. britannica*. However, they all evidence the presence of Al, Si, Sr, S, Cl, Ca, Mn and Fe. Some of them show the presence of K, Ti, V and Cr. In both set-up, the contribution from the Si_3N_4 window and ultralene membrane holding the nannofossils are shown in Fig. 1 and in Table 2.

At 17 keV, Mn is clearly and systematically recorded in the Bajocian species with a negligible contribution from the membrane. At 7.5 keV, Mn is clearly recorded in *D. striatus*, *W. britannica*, *D. araneus* and *C. pelagicus* and poorly in *H. carteri* (Fig. 2). The membranes contributions remain, in most case, negligible (Table 2).These contributions of Mn and other elements from the sample holders may come from the membranes themself, from the ethanol drop used during the picking procedure (Suchéras-Marx et al., 2016a) or residual elements leached from clay in the ethanol during the preparation.

3.2. Manganese maps

Both Ca and Mn elemental maps are presented for *D. striatus* and *W. britannica* analyzed at ID22 in Fig. 3 and for *D. striatus* and *W. britannica*, *D. araneus*, *C. leptoporus*, *H. carteri* and *C. pelagicus* analyzed at ID21 in Fig. 4. The Ca elemental map is considered hereafter as the reference for calcareous nannofossils calcite crystals organization and global shape. The high spatial resolution maps of *D. striatus* and *W. britannica* (Fig. 3) show that Mn is not homogeneously distributed. In both fossils, Mn distribution forms a ring with proximal/distal elongated structures that are directly comparable to the calcite crystals of the rim radiating in the R-unit of those placoliths (following R/V model from Young et al., 1992). The crystal shape and orientation are more easily observed in Mn maps than in Ca maps in both species. In species analyzed at ID21, the spatial resolution is high enough to clearly observe crystal organization for *D. araneus* on Ca and Mn maps (Fig. 4). In *D. araneus*, the central part is more concentrated in Ca than the rays, whereas Mn shows a maximal concentration in an intermediate region between the central knob and the rays. *D. striatus* and *W. britannica* evidence a distribution similar to the one observed in ID22 with ring-shape Mn distributions. *C. leptoporus* and *H. carteri* are depleted in Mn in comparison to the other species and the distribution is more homogeneous. Finally, in *C. pelagicus* conversely to *H. carteri* or *C. leptoporus*, the central area is easily identifiable on the Ca map, but is not observed in the Mn map. This coccolith is also more enriched in Mn, especially on one of his side clearly more concentrated in Mn, than both other core-top samples.

3.3. Mn K-edge XANES

The four analyzed coccoliths yielded similar Mn K-edge XANES spectra (Fig. 5). As a function of the investigated regions of *W. britannica*, the intensities of the peaks slightly differ but the positions of peaks remain similar (Supplementary Figure 1). All Mn XANES spectra of coccoliths present peaks which are very similar to the peaks of the $MnCO_3$ standard (Fig. 5). The pre-peak at 6.55 keV and the broad peak close to 6.56 keV are recorded on all coccoliths spectra. At higher energy, the peak above 6.57 keV is often recorded at slightly lower energy in coccoliths than in the standard. None of the coccoliths spectra display any characteristic peaks of $KMnO_4$ or MnO_2 (Fig. 5). This indicates that Mn is in the structure of the carbonate platelets and homogenously in the form of $MnCO_3$.

4. Discussion

The Ca maps represent the shape of analyzed coccoliths and thus allow a direct comparison of the crystalline organization and the Mn distribution. The Mn distribution is clearly different between fossil and recent samples. *D. striatus*, *W. britannica* and *D. araneus*, are from neither the same locality nor the same time interval. Nevertheless, they are both enriched in Mn compared to *C. pelagicus*, *C. leptoporus* and *H. carteri*. Mn is not randomly distributed in the fossil coccoliths but rather forms rings (Figs. 3-4). The fact that the crystals are more easily observed in Mn maps than Ca maps is related to the crystal growth direction. In Ca maps, both shields (i.e., a shield in placoliths is a disc formed by several calcite crystals) are superimposed, blurring the observation of crystals. However, the direction of crystals in Mn maps is perfectly clear because it corresponds to only one crystal growth direction thus to only one shield (Suchéras-Marx et al., 2016b). In the case of *D. araneus*, the center of the nannolith is less concentrated in Mn which corresponds to the thick central knob. Overall, Mn maps of all fossils display a distribution in close relation with the crystalline organization of the nannofossils. Conversely, the recent core-top samples are depleted in Mn with no clear organization observed. *C. pelagicus* is the only sample showing Mn enrichment, concentrated in one side of the coccolith. Unfortunately the limited spatial resolution does not support a discussion about the relation with the crystalline organization.

The XANES analyses clearly evidenced that, in all analyzed nannofossils, and the Mn is in the form of $MnCO_3$. Obviously, according to the XANES spectra and the XRF maps, in the nannofossils $CaCO_3$ there are substitutions of Ca by Mn to form $MnCO_3$ in small amount. XANES spectra did not evidenced contribution of oxidized Mn in our samples suggesting that Mn recorded in XRF maps did not come from surrounding organic matter or residual organic matter within the nannofossil crystals.

Firstly, the very low Mn concentrations in *C. leptoporus* and *H. carteri* show that coccolith primary calcite is depleted in Mn in well-preserved samples. This observation confirms that Mn concentration is too low to be a relevant biological or environmental proxy. Secondly, the Mn in nannofossils is more likely related to diagenesis and calcite crusts formation of slightly Mn-enriched carbonate precipitations. The calcite crust grows, in placoliths, following the crystal directions of one shield possibly in the interstice between both shields and/or on the distal shield (Suchéras-Marx et al., 2016a). In the case of *D. araneus*, the central knob is depleted in comparison to the border of the central region simply because diagenesis formed $CaCO_3$ crusts smoothing the nannofossil shape. Hence, the central knob is less covered in secondary diagenetic calcite than the rest of the nannolith. The secondary diagenetic calcite is generated by an interstitial fluid with high $[Ca^{2+}]$ and $[HCO_3^-]$ and slightly Mn^{2+}-enriched

thus with high potential of calcite precipitation on calcareous nannofossils. Our conclusion is coherent with previous chemical observations with secondary calcite crusts being depleted in Sr lowering the Sr/Ca (Dedert et al., 2014) and enriched in Mg (Prentice et al., 2014). The observation of Mn in calcareous nannfossils should then, like for foraminifera, be used as an indicator of diagenetic calcite crust (Boyle et al., 1983).

In the *C. pelagicus*, there is a relative higher content of Mn and localized enrichment which is related to another type of diagenetic enrichment than the one observed in *D. striatus*, *W. britannica* and *D. araneus*. Because *C. pelagicus* was sampled in a core-top, the enrichment was on the seafloor or maybe even in the water column and thus related to very early diagenesis encrusting processes and not to a late diagenesis like in rock samples' coccoliths. This early encrusting is related to the Northern Atlantic chemical particularities with i) high saturation state (i.e., $\Omega_{calcite}>1$; based on Lauvset et al., 2016) in the water column and at seafloor promoting calcite formation on calcite substrate like coccoliths and ii) high seawater [Mn^{2+}] in this region (van Hulten, et al., 2017). Such calcite encrusting is considered as a very early diagenesis that could be covered by secondary sedimentary diagenesis during rock formation. Potential early and later diagenesis may impact coccolith elemental composition and thus a careful check, even for recent material, is necessary before any geochemical analyses and could be done using Mn concentration measurements.

5. Conclusion

Coccoliths and other calcareous nannofossils are rarely used in paleoceanographical geochemistry due to their small size. Nevertheless, their long and abundant fossil record make them interesting geochemical substrates. In recent years, only the Sr/Ca ratio had been developed as a proxy of productivity. Mn being highly sensitive to oxidation, used in a key photosynthetic process, in high concentration in the oceans and easily permutable with Sr, it could be an interesting element to study. We show for the first time that Mn is enriched in nannofossils and depleted in recent coccoliths. The XANES analyses in the nannofossils show that Mn is in form of $MnCO_3$. Hence, the Mn in coccoliths is related to Mn-rich calcite crust covering calcareous nannofossils like in planktic foraminifera. A core-top coccolith was slightly enriched in Mn which would then argue for potential early diagenesis hence forcing, like for planktic foraminifera, to carefully check of coccoliths preservation, even for recent ones, before any geochemical analysis.

The calcareous nannofossil potential support for paleoceanographical reconstructions based on elemental geochemistry is only in its early days, recently developing due to the

development of analyzing tools allowing individual analyses or even elemental mapping. Even if Mn in calcareous nannofossil does not appear as an interesting element for paleoenvironmental or paleobiological reconstructions, ongoing research on Sr but also Mg (Prentice et al., 2014), S (Broche, 2018) or Cl (Suchéras-Marx et al., 2016b) are likely to lead to new paleoceanographical sea surface reconstructions, down to the Late Triassic. In this context, Mn will be a critical tool to estimate the chemical preservation of calcareous nannofossils.

Author contributions

BSM and FG designed the study with the contribution of ID and AS. BSM, FG, ID, AS, CR and RT conducted the analyses on both beamlines at ESRF whereas MPA, KHB and LB provided samples. BSM and AS performed the data treatment. BSM wrote the manuscript with comments from all contributors.

Acknowledgments

We acknowledge the ESRF for providing access to synchrotron radiation on ID21 and ID22NI beamlines (proposals EC-811 and ES-113).

Figures captions

Fig. 1: XRF spectra of *D. striatus* and *W. britannica* (17 keV). The black line corresponds to the whole nannofossil mean spectrum compared to the gray line which shows the contribution of the sample holder.

Fig. 2: XRF spectra of *D. striatus*, *W. britannica*, *D. araneus*, *C. leptoporus*, *H. carteri* and *C. pelagicus* (7.5 keV). The black line corresponds to the whole nannofossil mean spectrum whereas the gray line corresponds to the sample holder (Si_3N_4 window for *D. striatus* and *W. britannica*, ultralene foil for the others) mean spectrum.

Fig. 3: Ca and Mn maps of *D. striatus* and *W. britannica* (17 keV). Both intensity gray scales are in photon count per second.

Fig. 4: Ca and Mn maps of *D. striatus*, *W. britannica*, *D. araneus*, *C. leptoporus*, *H. carteri* and *C. pelagicus* (7.5 keV). Both intensity gray scales are in photon count per second.

Fig. 5: Mn K-edge XANES spectra of *D striatus*, *W. britannica*, *D. araneus* and *H carteri* compared to $KMnO_4$, MnO_2 and $MnCO_3$ standards. Dashed vertical lines are guides of the eyes to follow $MnCO_3$ characteristic spectroscopic features.

Table 1: Calcareous nannofossils species, sampling locality, age, type of nannofossil, type of sample holder and sample number.

Table 2: Membranes contributions (%) to the element concentration (in cps) in the calcareous nannofossils analyzed at 7.5 keV and 17 keV.

Supplementary Fig. 1: Mn K-edge XANES analyses of different parts of *W. britannica*, compared to $KMnO_4$, MnO_2 and $MnCO_3$ standards.

References

Bendif, E.M., Probert, I., Carmichel, M., Romac, S., Hagino, K., de Vargas, C., 2014. Genetic delineation between and within the widespread coccolithophore morpho-species *Emiliania huxleyi* and *Gephyrocapsa oceanica* (Haptophyta). J. Phycol. 50, 140-148.

Boyle, E.A., 1983. Manganese carbonate overgrowths on foraminifera tests. Geochim. Cosmochim. Ac. 47, 1815-1819.

Broche, B., 2018. L'impact du soufre sur le biocalcifiant *Emiliania huxleyi* (Prymnesiophyceae). Approches biogéochimiques liant l'Océan actuel et passé. Sorbonne Université, Paris.

Bruland, K.W., Lohan, C., 2003. Controls of trace metals in seawater, in: Elderfield, H. (Ed.), Treatise on Geochemistry. Elsevier, Amsterdam, pp. 23-47.

Cotte, M., Pouyet, E., Salomé, M., Rivard, C., De Nolf, W., Castillo-Michel, H., Fabris, T., Monico, L., Janssens, K., Wang, T., Sciau, P., Verger, L., Cormier, L., Dargaud, O., Brun, E., Bugnazet, D., Fayard, B., Hesse, B., Pradas del Real, A.E., Veronesi, G., Langlois, J., Balcar, N., Vandenberghe, Y., Solé, V.A., Kieffer, J., Barrett, R., Cohen, C., Cornu, C., Baker, R., Gagliardini, E., Papillon, E., Susini, J., 2017. The ID21 X-ray and infrared microscopy beamline at the ESRF: status and recent applications to artistic materials. J. Anal. Atom. Spectrom. 32, 477-493.

Dedert, M., Stoll, H.M., Kars, S., Young, J.R., Shimizu, N., Kroon, D., Lourens, L.J., Ziveri, P., 2014. Temporally variable diagenetic overgrowth on deep-sea nannofossil carbonates

341 across Palaeogene hyperthermals and implications for isotopic analyses. Mar.
342 Micropaleontol. 107, 18-31.
343 Dismukes, G.C., van Willigen, R.T., 2006. Manganese: The Oxygen-Evolving Complex &
344 Models Based in part on the article Manganese: Oxygen-Evolving Complex & Models by
345 Lars-Erik Andréasson & Tore Vänngård which appeared in the Encyclopedia of Inorganic
346 Chemistry, First Edition, in: King, R.B., Crabtree, R.H., Lukehart, C.M., Atwood, D.A.,
347 Scott, R.A. (Eds.), Encyclopedia of Inorganic Chemistry, Wiley.
348 Gardin, S., Krystyn, L., Richoz, S., Bartolini, A., Galbrun, B., 2012. Where and when the
349 earliest coccolithophores? Lethaia 45, 507-523.
350 Hermoso, M., Lefeuvre, B., Minoletti, F., de Rafélis, M., 2017. Extreme strontium
351 concentrations reveal specific biomineralization pathways in certain coccolithophores with
352 implications for the Sr/Ca paleoproductivity proxy. Plos One 12, e0185655.3
353 Ho, T.-Y., Quigg, A., Finkel, Z.V., Milligan, A.J., Wyman, K., Falkowski, P.G., Morel,
354 F.M.M., 2003. The elemental composition of some marine phytoplankton. J. Phycol. 39,
355 1145-1159.
356 Lauvset, S.K., Key, R.M., Olsen, A., van Heuven, S., Velo, A., Lin, X., Schirnick, C., Kozyr,
357 A., Tanhua, T., Hoppema, M., Jutterström, S., Steinfeldt, R., Jeansson, E., Ishii, M., Perez,
358 F.F., Suzuki, T., Watelet, S., 2016. A new global interior ocean mapped climatology: the
359 1° × 1° GLODAP version 2. Earth Syst. Sci. Data 8, 325-340.
360 Paquette, J., Reeder, R.J., 1995. Relationship between surface structure, growth mechanism,
361 and trace element incorporation in calcite. Geochim. Cosmochim. Ac. 59, 735-749.
362 Pavia, G., Enay, R., 1997. Definition of the Aalenian-Bajocian Stage boundary. Episodes 20,
363 16-22.
364 Pena, L.D., Cacho, I., Calvo, E., Pelejero, C., Eggins, S., Sadekov, A., 2008. Characterization
365 of contaminant phases in foraminifera carbonates by electron microprobe mapping.
366 Geochem. Geophy. Geosy. 9, Q07012.
367 Prentice, K., Dunkley Jones, T., Lees, J., Young, J.R., Bown, P.R., Langer, G., Fearn, S.,
368 EIMF, 2014. Trace metal (Mg/Ca and Sr/Ca) analyses of single coccoliths by Secondary
369 Ion Mass Spectrometry. Geochim. Cosmochim. Ac.146, 90-106.
370 Reinhardt, P., Coccolithen. Kalkiges Plankton seit Jahrmillionen. Die Neue Brehm-Bücherei,
371 A. Ziemsen Verlag, Lutherstadt Wittenberg 453.
372 Siesser, W.G., 1977. Chemical composition of calcareous nannofossils. S. Afr. J. Sci. 73, 283-
373 285.

Stoll, H.M., Schrag, D.P., 2000. Coccolith Sr/Ca as a new indicator of coccolithophorid calcification and growth rate. Geochim. Cosmochim. Ac. 1, 1006.

Stoll, H.M., Shimizu, N., 2009. Micropicking of nannofossils in preparation for analysis by secondary ion mass spectrometry. Nat. Protoc. 4, 1038-1043.

Stoll, H.M., Encinar, J.R., Alonso, J.I.G., Rosenthal, Y., Probert, I., Klaas, C., 2001. A first look at paleotemperature prospects from Mg in coccolith carbonate: Cleaning techniques and culture measurements. Geochem. Geophy. Geosy. 2, 2000GC000144.

Stoll, H.M., Rosenthal, Y., Falkowski, P., 2002a. Climate proxies from Sr/Ca of coccolith calcite: calibrations from continuous culture of *Emiliania huxleyi*. Geochim. Cosmochim. Ac. 66, 927-936.

Stoll, H.M., Ziveri, P., Geisen, M., Probert, I., Young, J.R., 2002b. Potential and limitations of Sr/Ca ratios in coccolith carbonate: new perspectives from cultures and monospecific samples from sediments. Philos. Troy. Soc. A 360, 719-747.

Stoll, H.M., Shimizu, N., Arevalos, A., Matell, N., Banasiak, A., Zeren, S., 2007. Insights on coccolith chemistry from a new ion probe method for analysis of individually picked coccoliths. Geochem. Geophy. Geosy. 8, Q06020.

Suchéras-Marx, B., Guihou, A., Giraud, F., Lécuyer, C., Allemand, P., Pittet, B., Mattioli, E., 2012. Impact of the Middle Jurassic diversification of *Watznaueria* (coccolith-bearing algae) on the carbon cycle and $\delta^{13}C$ of bulk marine carbonates. Global Planet. Change 86-87, 92-100.

Suchéras-Marx, B., Giraud, F., Lena, A., Simionovici, A., 2016a. Picking nannofossils: How and why. J. Micropalaeontol. 36, 219-221.

Suchéras-Marx, B., Giraud, F., Simionovici, A., Daniel, I., Tucoulou, R., 2016b. Perspectives on heterococcolith geochemical proxies based on high-resolution X-ray fluorescence mapping. Geobiology 14, 390-403.

Suchéras-Marx, B., Mattioli, E., Allemand, P., Giraud, F., Pittet, B., Plancq, J., Escarguel, G., 2019. The colonization of the oceans by calcifying pelagic algae. Biogeosciences 16, 2501-2510.

van Hulten, M., Middag, R., Dutay, J.C., de Baar, H., Roy-Barman, M., Gehlen, M., Tagliabue, A., Sterl, A., 2017. Manganese in the west Atlantic Ocean in the context of the first global ocean circulation model of manganese. Biogeosciences 14, 1123-1152.

Winter, A., Jordan, R.W., Roth, P.H., 1994. Biogeography of living coccolithophores in ocean waters, in: Winter, A., Siesser, W.G. (Eds.), Coccolithophores. Cambridge University Press, Cambridge, 161-178.

408 Young, J.R., Didymus, J.M., Bown, P.R., Mann, S., 1992. Crystal assembly and phylogenetic
409 evolution in heterococcoliths. Nature 356, 516-518.

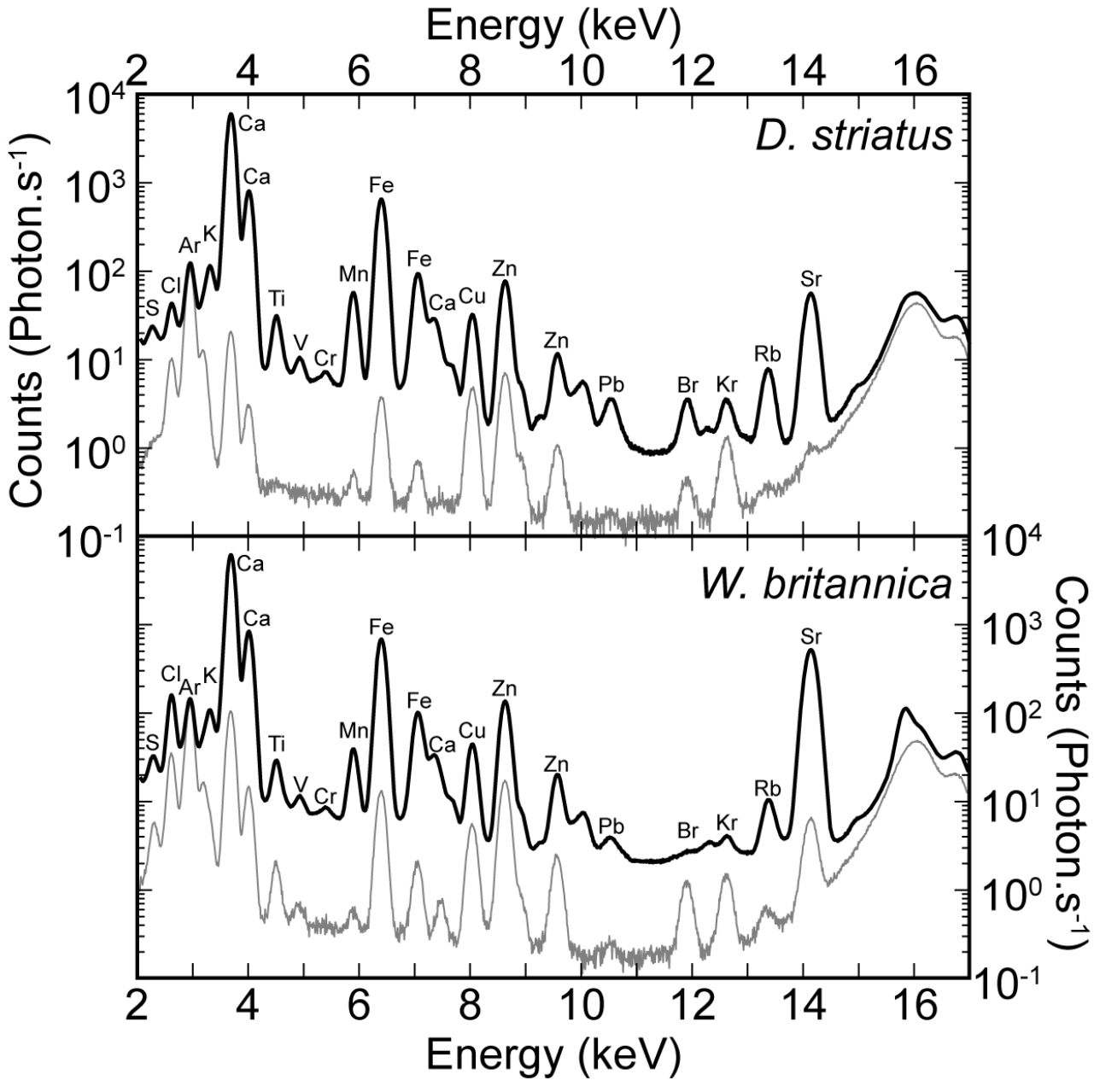
Energy (keV)
Counts (Photon.s-1)
D. striatus
W. britannica
S
Cl
Ar
K
Ca
Ti
V
Cr
Mn
Fe
Ca
Cu
Zn
Pb
Br
Kr
Rb
Sr

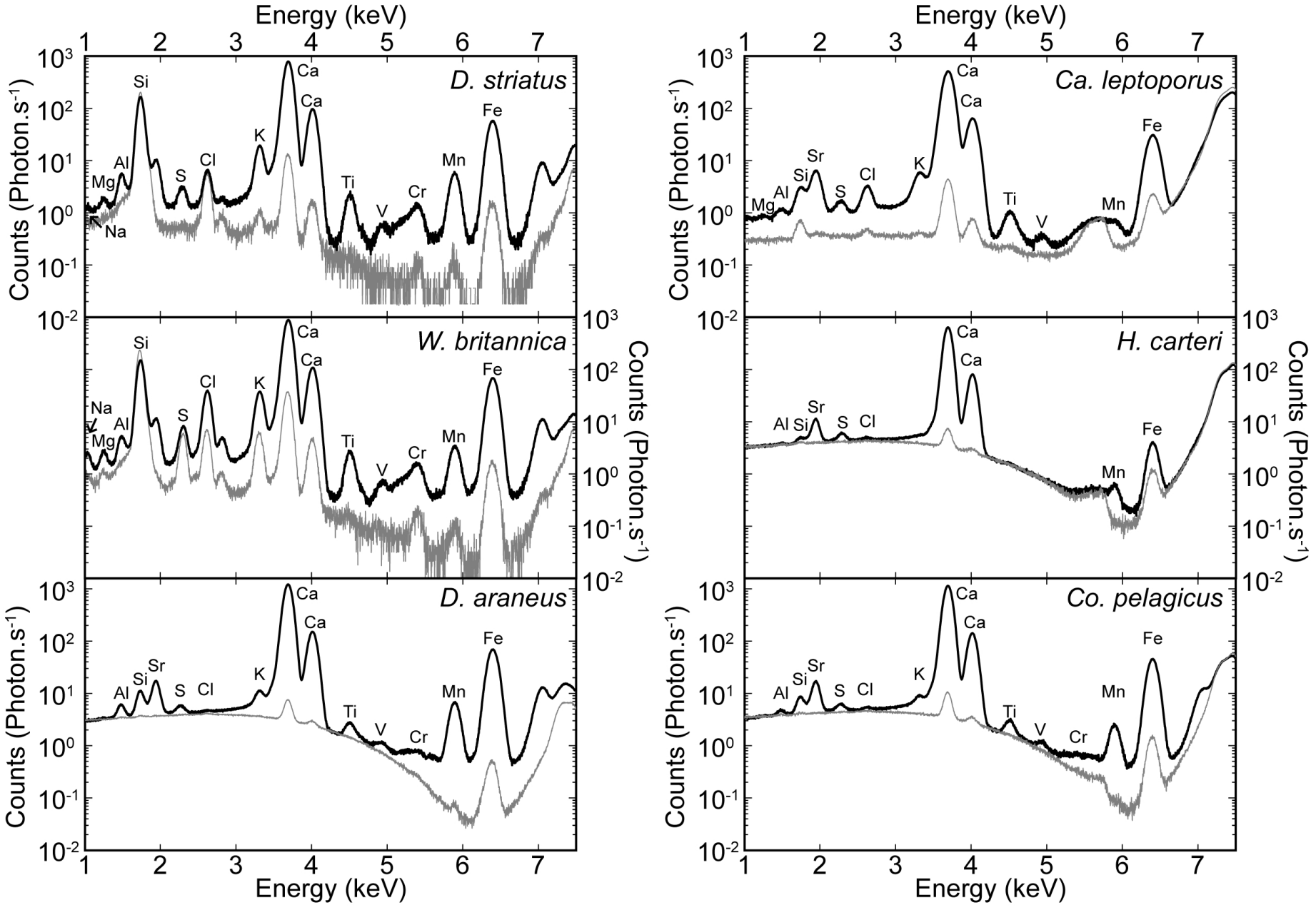
Energy (keV)
Counts (Photon.s-1)
D. striatus
W. britannica
D. araneus
Ca. leptoporus
H. carteri
Co. pelagicus
Mg
Al
Si
Na
S
Cl
K
Ca
Ti
V
Cr
Mn
Fe
Sr

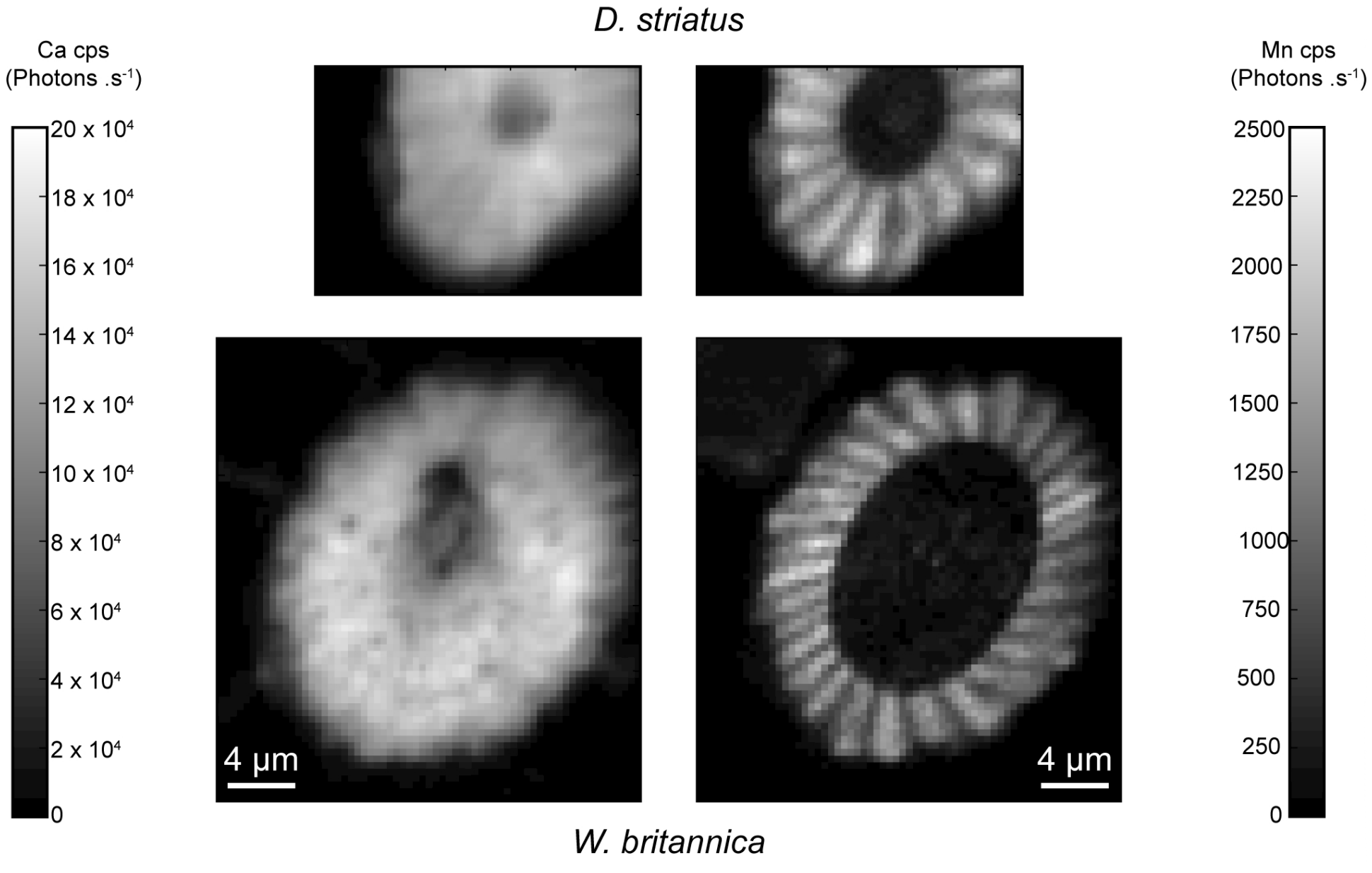
D. striatus
Ca cps
(Photons .s-1)
20 x 10⁴
18 x 10⁴
16 x 10⁴
14 x 10⁴
12 x 10⁴
10 x 10⁴
8 x 10⁴
6 x 10⁴
4 x 10⁴
2 x 10⁴
0
Mn cps
(Photons .s-1)
2500
2250
2000
1750
1500
1250
1000
750
500
250
0
4 µm
4 µm
W. britannica

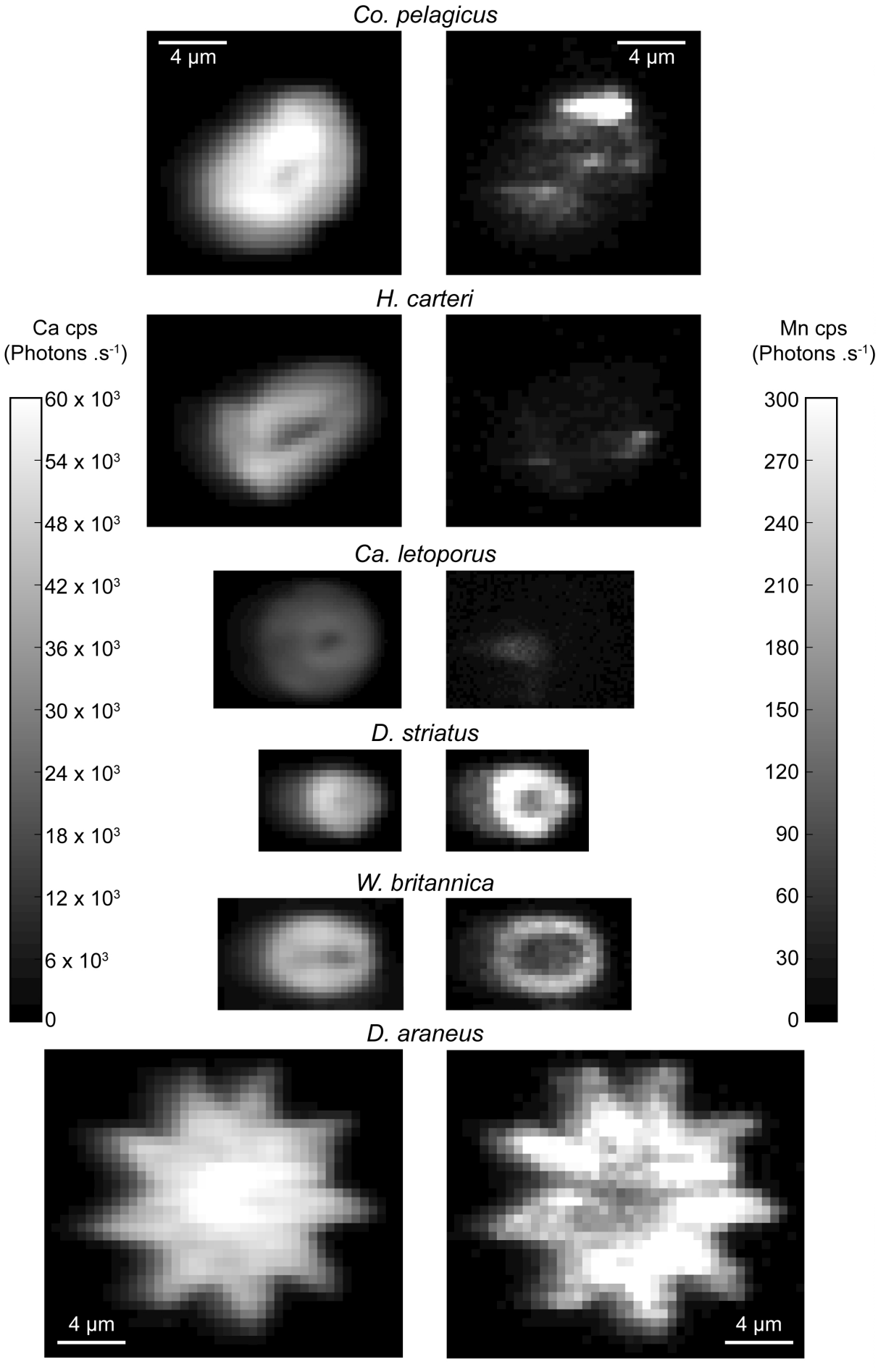
Co. pelagicus
4 µm
4 µm
H. carteri
Ca cps
(Photons .s-1)
60 x 10³
54 x 10³
48 x 10³
42 x 10³
36 x 10³
30 x 10³
24 x 10³
18 x 10³
12 x 10³
6 x 10³
0
Mn cps
(Photons .s-1)
300
270
240
210
180
150
120
90
60
30
0
Ca. letoporus
D. striatus
W. britannica
D. araneus
4 µm
4 µm

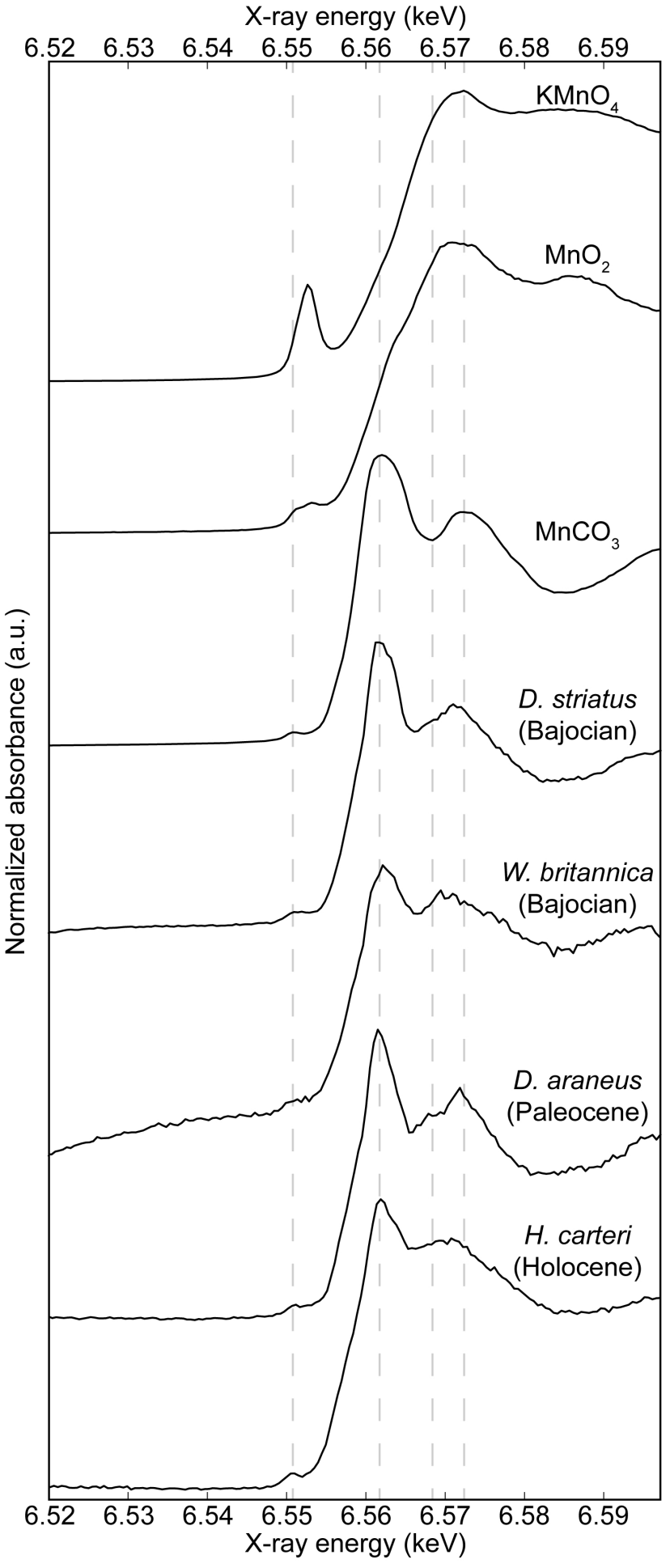
X-ray energy (keV)
6.52
6.53
6.54
6.55
6.56
6.57
6.58
6.59
KMnO4
MnO2
MnCO3
D. striatus
(Bajocian)
W. britannica
(Bajocian)
D. araneus
(Paleocene)
H. carteri
(Holocene)
Normalized absorbance (a.u.)
6.52
6.53
6.54
6.55
6.56
6.57
6.58
6.59
X-ray energy (keV)

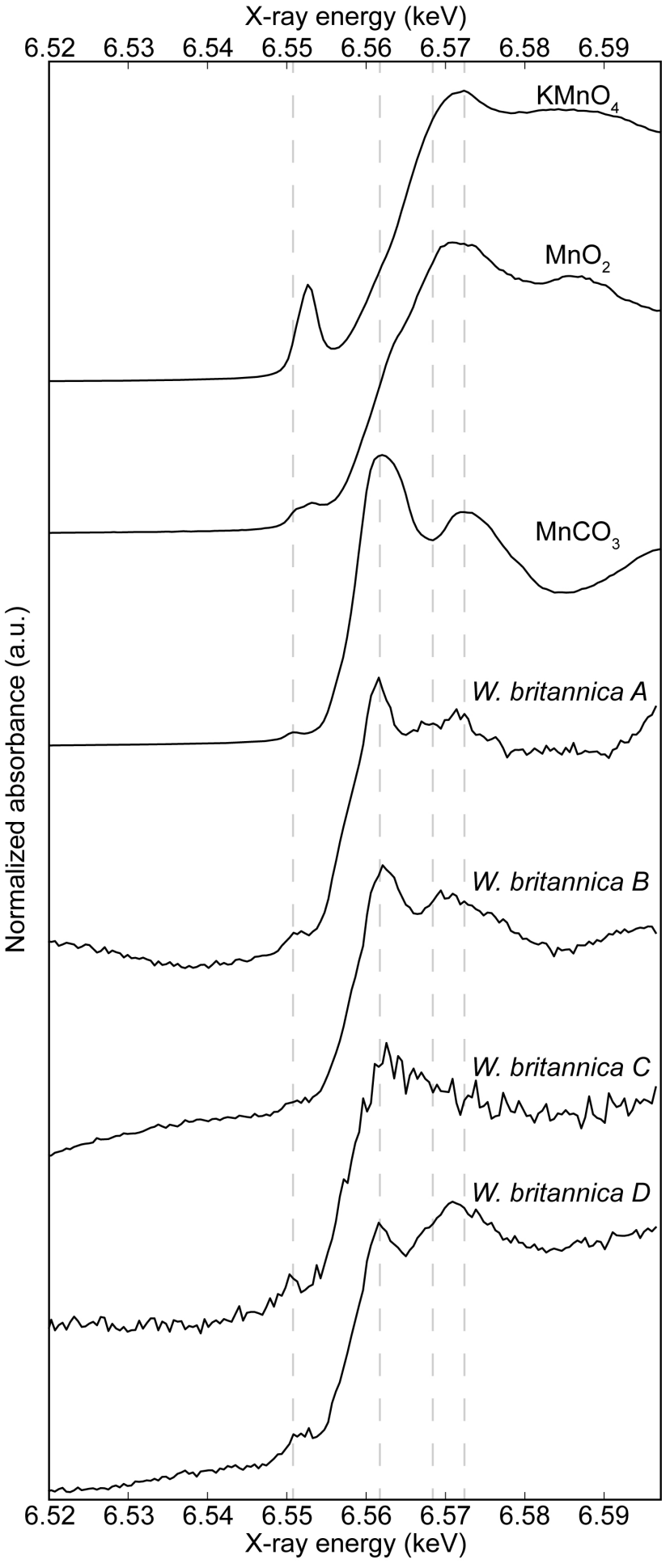
X-ray energy (keV)
6.52
6.53
6.54
6.55
6.56
6.57
6.58
6.59
KMnO4
MnO2
MnCO3
W. britannica A
W. britannica B
W. britannica C
W. britannica D
Normalized absorbance (a.u.)
6.52
6.53
6.54
6.55
6.56
6.57
6.58
6.59
X-ray energy (keV)

Species	Locality	Age	type of nannofossil	Sample holder	Sample number
Discorhabdus striatus	Cabo Mondego, Portugal	Lower Bajocian, Jurassic	placolith	500 nm-thick Si_3N_4 window	CM60
Watznaueria britannica	Cabo Mondego, Portugal	Lower Bajocian, Jurassic	placolith	500 nm-thick Si_3N_4 window	CM9
Discoaster araneus	Wilson lake, USA	Paleogene	multiradiate nannolith	4 µm-thick ultralene	n/a
Calcidiscus leptoporus	South Atlantic core-top	recent	placolith	4 µm-thick ultralene	GeoB3721-4
Coccolithus pelagicus	Norwegian sea core-top	recent	placolith	4 µm-thick ultralene	GIK23066
Helicosphaera carteri	South Atlantic core-top	recent	placolith	4 µm-thick ultralene	GeoB3721-4
Helicosphaera carteri	Equatorial West Pacific core-top	recent	placolith	4 µm-thick ultralene	MD052920

	D. striatus / W. britannica		*D. araneus*	*C. leptoporus*	*C. pelagicus*	*H. carteri*
Membrane contribution (%)	17 keV	7.5 keV	7.5 keV	7.5 keV	7.5 keV	7.5 keV
>1	S, Cl, Cu, Zn, Br	Na, Mg, Al, S, Cl, K	Al, Si, S, K, Ti, V, Cr	Mg, Al, Si, S, Cl, K, Ti, V, Mn	Al, Si, S, K, Ti, V, Cr	Al, Si, S, Cl, Mn, Fe
<1	K, Ca, Ti, V, Cr, Mn, Fe, Rb, Sr	Ca, Ti, Cr, Mn, Fe	Ca, Mn, Fe	Ca, Fe	Ca, Mn, Fe	Ca